The Journal of Chemical Physics

A potential for molecular simulation of compounds with linear moieties

Cite as: J. Chem. Phys. **153**, 084503 (2020); https://doi.org/10.1063/5.0015184
Submitted: 27 May 2020 . Accepted: 12 August 2020 . Published Online: 26 August 2020

David van der Spoel, Henning Henschel, Paul J. van Maaren, Mohammad M. Ghahremanpour, and Luciano T. Costa

The Journal of Chemical Physics ARTICLE scitation.org/journal/jcp

A potential for molecular simulation of compounds with linear moieties

Cite as: J. Chem. Phys. 153, 084503 (2020); doi: 10.1063/5.0015184
Submitted: 27 May 2020 • Accepted: 12 August 2020 •
Published Online: 26 August 2020

David van der Spoel,[1,a)] Henning Henschel,[1] Paul J. van Maaren,[1] Mohammad M. Ghahremanpour,[2] and Luciano T. Costa[3]

AFFILIATIONS

[1]Science for Life Laboratory, Department of Cell and Molecular Biology, Uppsala University, Box 596, SE-75124 Uppsala, Sweden
[2]Chemistry Department, Yale University, New Haven, Connecticut 06520 8107, USA
[3]MolMod-CS - Instituto de Química, Universidade Federal Fluminense, Niterói, RJ CEP 24020-141, Brazil

Note: This paper is part of the JCP Special Topic on Classical Molecular Dynamics (MD) Simulations: Codes, Algorithms, Force Fields, and Applications.
[a)]**Author to whom correspondence should be addressed:** david.vanderspoel@icm.uu.se

ABSTRACT

The harmonic angle bending potential is used in many force fields for (bio)molecular simulation. The force associated with this potential is discontinuous at angles close to 180°, which can lead to numeric instabilities. Angle bending of linear groups, such as alkynes or nitriles, or linear molecules, such as carbon dioxide, can be treated by a simple harmonic potential if we describe the fluctuations as a deviation from a reference position of the central atom, the position of which is determined by the flanking atoms. The force constant for the linear angle potential can be derived analytically from the corresponding force constant in the traditional potential. The new potential is tested on the properties of alkynes, nitriles, and carbon dioxide. We find that the angles of the linear groups remain about 2° closer to 180° using the new potential. The bond and angle force constants for carbon dioxide were tuned to reproduce the experimentally determined frequencies. An interesting finding was that simulations of liquid carbon dioxide under pressure with the new flexible model were stable only when explicitly modeling the long-range Lennard-Jones (LJ) interactions due to the very long-range nature of the LJ interactions (>1.7 nm). In the other tested liquids, we find that a Lennard-Jones cutoff of 1.1 nm yields similar results as the particle mesh Ewald algorithm for LJ interactions. Algorithmic factors influencing the stability of liquid simulations are discussed as well. Finally, we demonstrate that the linear angle potential can be used in free energy perturbation calculations.

I. INTRODUCTION

Most molecular simulation programs implement an angle bending potential V_θ that depends harmonically on the angle θ formed by the three atoms, e.g., H–O–H in water,

$$V_\theta = \frac{k_\theta}{2}\left(\theta - \theta^0\right)^2, \tag{1}$$

where the reference angle θ^0 and the force constant k_θ may be derived from spectroscopy experiments or from quantum chemistry calculations. The force on any of the three involved atoms i, j, k, e.g., for atom i,

$$\mathbf{F}_i = -\frac{\partial V}{\partial \mathbf{r}_i} = k_\theta\left(\theta - \theta^0\right)\frac{\partial \theta}{\partial \mathbf{r}_i} \tag{2}$$

for this potential is ill-defined in case the angle is 180°. The reason for this is that the angle

$$\theta = \arccos\left(\frac{\mathbf{r}_{ij}\cdot\mathbf{r}_{kj}}{\|r_{ij}\|\|r_{kj}\|}\right) \tag{3}$$

and

$$\frac{\partial \arccos(x)}{\partial x} = -\frac{1}{\sqrt{1-x^2}}, \tag{4}$$

which is undefined as $x \to \pm 1$. This problem is, in particular, important for linear chemical moieties, such as nitrile groups, or compounds, such as carbon dioxide. Some programs, such as the Antechamber toolkit,[1] use a workaround by setting the angle of linear groups to ≈178°. Simulation engines, such as GROMACS,[2–5] implement a construction using virtual sites[6] where, in the case of carbon dioxide, one would add two virtual particles, the distance between which is constrained and from which the three atomic positions are generated. The constructed atoms cannot carry any mass, and therefore, the two virtual particles carry the mass and have to be situated at a position to maintain the correct moment of inertia of the CO_2 molecule. While the use of virtual sites leads to stable simulations, it also removes a degree of freedom, which is not necessarily fast and therefore may be significant in order to reproduce vibration-dependent properties such as entropy and heat capacities.[7] Furthermore, virtual sites are inconvenient since they, in general, introduce extra "particles" that confuse graphics programs, demand a higher computational cost, and lead to code complexity, in particular, for parallel simulation engines. It should be noted here that a number of different angle potentials are in use predominantly based on $\cos(\theta)$ and potentials with higher order in θ in order to model the true anharmonic behavior of angle bending. However, there is considerable advantage to a true harmonic potential, the most important being that its properties are known analytically in most cases.

In a recent series of force field benchmark papers,[7–12] we have reported simulations of a number of organic molecules containing nitrile groups treated using both the Antechamber approach, for simulations based on the General Amber force field,[13] and optimized potential for liquid simulation with all atoms (OPLS/AA);[14] in the latter case, we implemented virtual sites for the simulation of linear compounds. In addition, we used the Charmm General force field[15] for determining gas-phase entropy and heat capacity from force fields[7] and compared those to the quantum-chemical calculations[16] that are available in the Alexandria library.[17] More recently, we looked into the predictions of infrared spectra from these force fields and found alkynes to be a problematic group.[18,19]

The focus in this paper is on a new potential for linear angles which we describe below and applications to a series of 16 compounds with linear groups for which experimental spectra are available in the National Institute of Standards database.[20] We provide the results from gas-phase standard entropy and heat capacity calculations, and from simulations of liquids and of hydration free energy perturbation calculations with both the traditional and linear angle potentials.

II. THEORY

A. Energy function

The reference position, corresponding to a minimum energy structure, $\boldsymbol{x}_j^0$ for a central atom j in a linear triplet of atoms i, j, k is given by

$$\boldsymbol{x}_j^0 = \mathrm{a}\,\boldsymbol{x}_i + (1-\mathrm{a})\,\boldsymbol{x}_k, \tag{5}$$

where a is a constant defined by the bond lengths $i-j$ and $j-k$. For instance, in carbon dioxide and other symmetric molecules, one would have $a = 1/2$. In a group with bonds $i-j$ and $j-k$ with lengths b_{ij} and b_{jk}, respectively, the constant would follow from

$$a = \frac{b_{jk}}{b_{ij}+b_{jk}}. \tag{6}$$

Note that if the order of atoms is flipped from $i-j-k$ to $k-j-i$, a will change as well. The potential V_{lin} is then given by

$$V_{lin} = \frac{\mathrm{k}_{lin}}{2}\left(\boldsymbol{x}_j - \boldsymbol{x}_j^0\right)^2, \tag{7}$$

with k_{lin} being the force constant. If we substitute Eq. (5) and take the negative derivative, we obtain the forces on the atoms

$$\boldsymbol{F}_i = \mathrm{a}\,\mathrm{k}_{lin}(\boldsymbol{x}_j - \mathrm{a}\,\boldsymbol{x}_i - (1-\mathrm{a})\,\boldsymbol{x}_k), \tag{8}$$

$$\boldsymbol{F}_k = (1-\mathrm{a})\,\mathrm{k}_{lin}(\boldsymbol{x}_j - \mathrm{a}\,\boldsymbol{x}_i - (1-\mathrm{a})\,\boldsymbol{x}_k), \tag{9}$$

$$\boldsymbol{F}_j = -\boldsymbol{F}_i - \boldsymbol{F}_k. \tag{10}$$

The above equations were implemented in the GROMACS software[2–5] and have been part of the regular release from version number 4.6 but have not been reported previously. For completeness, we mention that the above potential can be used in free energy perturbation calculations by making it dependent on a parameter λ that can be varied from 0 to 1 corresponding to different states A and B. This is described in Sec. II C.

B. Force constants

Angular force constants k_θ can be converted into linear ones k_{lin} by the following argument: the force constants should be identical close to the equilibrium position. We write x_j using the cosine rule,

$$(b_{ij}+b_{jk})^2 = b_{ij}^2 + b_{jk}^2 - 2b_{ij}b_{jk}\cos\theta, \tag{11}$$

in terms of θ and the bond lengths b_{ij} and b_{jk}, insert that into Eq. (7), and take the second derivative with respect to θ. If we then take the limit of θ going to zero, we can equate the result to the original force constant,

$$\mathrm{k}_\theta = \frac{\partial^2 V_{lin}}{\partial\theta^2} = \mathrm{k}_{lin}\frac{b_{ij}^2\,b_{jk}^2}{2(b_{ij}+b_{jk})^2}. \tag{12}$$

For example, Huang *et al.* used a force constant $\mathrm{k}_\theta = 236.5$ kJ/(mol rad^2) for carbon dioxide bending.[21] Since the C=O bond length in carbon dioxide is 0.1149 nm, the corresponding linear force constant should be $\mathrm{k}_{lin} = 8\mathrm{k}_\theta/b^2 = 143\,312$ kJ/(mol nm^2). With this force constant, we reproduce the frequency of 680 cm^{-1} published by Huang *et al.*;[21] however, here, we have tuned the force constants for carbon dioxide such that we reproduce all three measured frequencies exactly[22] (see Sec. III).

C. Free energy perturbation

In order to compute free energies for changing a molecule from state A to B, we introduce

$$k_{lin}(\lambda) = k_{lin}^{A}(1-\lambda) + k_{lin}^{B}\lambda, \tag{13}$$

$$a(\lambda) = a^{A}(1-\lambda) + a^{B}\lambda, \tag{14}$$

and

$$\boldsymbol{x}_0(\lambda) = a(\lambda)\boldsymbol{x}_i - (1-a(\lambda))\boldsymbol{x}_k. \tag{15}$$

Using these equations, one can derive the derivative of the potential with respect to λ,

$$\frac{\partial V(\lambda)}{\partial \lambda} = \frac{1}{2}(k_B - k_A)(\boldsymbol{x}_j - \boldsymbol{x}_0(\lambda))^2 + (k_A(1-\lambda) + k_B\lambda) \times (a_B - a_A)(\boldsymbol{x}_j - \boldsymbol{x}_0(\lambda)) \cdot (\boldsymbol{x}_k - \boldsymbol{x}_i). \tag{16}$$

In principle, one could write the λ-dependency of a as dependent on the bond lengths [Eq. (6)]; however, since the free energy is a state function, the exact path from A to B does not matter, and therefore, the simpler λ dependence of a as given in Eq. (14) was implemented instead. An evaluation of the free energy code is given in the supplementary material, Sec. II.

III. METHODS

Sixteen compounds (Table I) were taken from a recent study where we compared the infrared spectra computed using force fields and density functional theory to experimental data.[18] As a reference, we used the CGenFF models[15,23,24] for these compounds that we used in recent studies as well.[7,18] For two of the compounds, methyl-isocyanate and methyl-isothiocyanate that have two double bonds in a row, the angle in the topology had to be corrected to 180° as it had been generated incorrectly. In addition, the central C–C bond in cyanoacetylene was incorrectly assigned to a bond length corresponding to a triple bond. Based on the bond length due to B3LYP/aug-cc-pVTZ calculation from the Alexandria library,[17] a bond length of 0.1368 nm was assigned to this bond. For all compounds, we converted the harmonic angle force constant k_θ to k_{lin} using Eq. (12), whereas the proportionality constant a was derived from the bond lengths using Eq. (6). The resulting values are given in Table I.

For carbon dioxide, a new model was generated based on the following ansatz: the geometry optimized at the B3LYP/aug-cc-pVTZ level of theory was taken from the Alexandria library.[17,25] 500 off-equilibrium structures were generated using a script varying both bond lengths and angles. For each of these conformations, a single point energy calculation was done using Gaussian 16[26] at the same level of theory, and the energy relative to the optimized geometry was stored. The distribution of energies ranged from 0 kJ/mol to 70 kJ/mol. Then, a model using harmonic bonds, a linear angle, and a Urey–Bradley term was fitted using a grid search. The three-parameter model reproduces the energy distribution from density functional theory with a root-mean-square deviation of just under 2 kJ/mol (Fig. 1). The intermolecular parameters from CGenFF were left unchanged. It can be noted (Table II) that the k_{lin} is quite close to the value based on the work of Huang *et al.*[21] These updated models, here called CGenFF-linear, will be

TABLE I. Test compounds used and angle force constants. k_θ taken from CGenFF and k_{lin} based on Eq. (12). Relative position of the central atom *a* from Eq. (6).

Compound	Formula	Angle	k_θ kJ/(mol rad^2)	k_{lin} kJ/(mol nm^2)	*a*
2-butyne	C_4H_6	C–C≡C	158.99	71 763	0.454 376
2-propyn-1-ol	C_3H_4O	C≡C–C	92.05	41 547	0.545 624
		C≡C–H	66.9	41 202.7	0.467 249
2-thiophene-carbonitrile	C_5H_3NS	C–C≡N	334.7	160 977	0.453 497
2,2-dimethylpropanenitrile	C_5H_9N	C–C≡N	177.4	82 810	0.445 283
3-methoxypropanenitrile	C_4H_7NO	C–C≡N	177.4	82 810	0.445 283
3,3-dimethyl-1-butyne	C_6H_{10}	C–C≡C	92.05	41 546.8	0.454 376
		C≡C–H	66.9	41 202.7	0.467 249
4-pyridinecarbonitrile	$C_6H_4N_2$	C–C≡N	334.7	160 977	0.453 497
Acetonitrile	C_2H_3N	C–C≡N	177.4	82 810	0.445 283
Benzonitrile	C_7H_5N	C–C≡N	334.7	160 977	0.453 497
Carbon dioxide[a]	CO_2	O=C=O	376.5	220 066	0.500 000
Cyanoacetylene	C_3HN	N≡C–C	334.7	166 791.6	0.536 892
		C–C≡C	92.05	44 267.1	0.471 406
		C≡C–H	66.9	41 202.7	0.467 249
Cyclobutanenitrile	C_5H_7N	C–C≡N	177.4	82 810	0.445 283
Hexa-1,5-diyne	C_6H_6	C–C≡C	92.05	41 546.8	0.454 376
		C≡C–H	66.9	41 202.7	0.467 249
Methyl-isocyanate	C_2H_3NO	O=C=N	351.4	201 957	0.504 237
Methyl-isothiocyanate	C_2H_3NS	S=C=N	351.4	148 569	0.421 986
Propanenitrile	C_3H_5N	C–C≡N	177.4	82 810	0.445 283

[a]For the optimized parameters, see Table II.

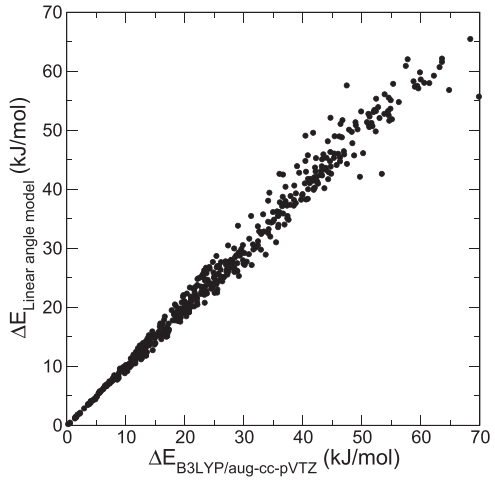

FIG. 1. Correlation between energy from density functional theory and the linear-angle model for carbon dioxide.

published as part of the GROMACS molecule & liquid database[9] at http://virtualchemistry.org.

Simulations were performed using GROMACS 2019. The detailed procedure of these simulations is available in our previous papers.[8,10] In short, cubic boxes of 1000 molecules were built for liquid simulations using the Packmol program[27,28] and a single molecule in a box for a gas-phase simulation. All these simulations used constraints on bonds involving hydrogen, rather than flexible bonds, as implemented using the parallel LINCS algorithm.[29] All condensed-phase simulations used the particle-mesh Ewald algorithm for computation of the electrostatic forces[30] with a real-space cutoff of 1.1 nm. Lennard-Jones interactions were treated with either a smooth cut-off with analytical corrections to energy and pressure,[31] or, in separate simulations, Lennard-Jones particle mesh-Ewald (PME)[30,32] since some of the simulations, in particular of CO_2 were unstable with Lennard-Jones cutoffs. In production simulations, initially, the Nosé–Hoover temperature coupling algorithm[33,34] was used combined with the Parrinello–Rahman pressure coupling algorithm[35] with time constants of 0.5 ps and 5 ps, respectively. However, because simulations of some compounds were difficult to equilibrate, another set of liquid simulations was done using the Berendsen barostat[36] with a time constant of 5 ps, combined with the velocity rescaling thermostat[37] with a time constant of 0.5 ps.

TABLE II. Intramolecular force field parameters for the new carbon dioxide model.

Parameter	Value
r_{CO}	0.116 1 nm
k_b	770 200 kJ/(mol nm^2)
k_{UB}	164 800 kJ/(mol nm^2)
k_{lin}	139 600 kJ/(mol nm^2)

Carbon dioxide is liquid only at elevated pressures. Here, we simulated it at 50 bars, 100 bars, and 200 bars, and at temperatures of 225 K and 250 K. For these simulations, the temperature coupling time was 1 ps, and the pressure coupling time was 50 ps. We found that the liquid carbon dioxide simulations were unstable with a relatively short Lennard-Jones cutoff of 1.1 nm (see the supplementary material for details). Since equilibration was very slow, 250 ns were simulated and averaged taken over the last 50 ns.

Free energy perturbation was evaluated by solvating methyl-isocyanate in a box containing 2000 TIP3P water molecules[38] and running an equilibration in the same manner as the liquid simulation for 10 ns. Then, the $\partial H/\partial\lambda$ was sampled according to Eq. (16) at 11 λ values, regularly spaced from 0 to 1, mutating the compound into methyl-isothiocyanate. At each λ, 100 ps of simulations were done of which the first 20 ps were discarded as equilibration. Before the sampling, a steepest descent energy minimization was performed. The procedure was done using both the harmonic- and linear-angle potentials.

IV. RESULT AND DISCUSSION

A. Gas-phase infrared spectra

The infrared spectra for all compounds were computed as described in a recent paper.[18] They are plotted in Fig. 2 using both the traditional angle potential and the linear angle potential with an experimental reference. The infrared spectra produced by force fields are much less accurate than those produced by density functional theory, and this can become a very effective benchmark for future force fields.[19] This is somewhat cumbersome since early force fields were parameterized with much more focus on reproducing experimental vibrations.[39]

B. Thermochemistry

Standard entropies S^0 and heat capacities at constant volume C_V were computed for all compounds, as detailed by van der Spoel *et al.*,[7] and the resulting values are listed in Table III. First, we note that the hand-tuned carbon dioxide model exactly reproduces the experimental values for standard entropy and almost exactly the heat capacity at constant volume. These properties are derived from the vibrational frequencies, and the model was fitted to the potential energy surface (PES) at the B3LYP/aug-cc-pVTZ level of theory, so it is encouraging to observe that the intramolecular PES from density functional theory is consistent with the experimental numbers. A general observation is that replacing the traditional harmonic potential by the linear angle potential leads to slightly reduced S^0 and C_V.

C. Liquid simulations

The distribution of angles of linear moieties in the liquid phase differs clearly between the two potentials, with the linear potential remaining closer to 180° in all cases (Fig. 3) with an average difference of about 2° (Table S4). Although this intuitively seems desirable, it would require detailed comparison with liquid structural data from, e.g., scattering experiments.

The liquid density for the 15 liquids is given in Table S2 with, where available, experimental data. The differences between the two

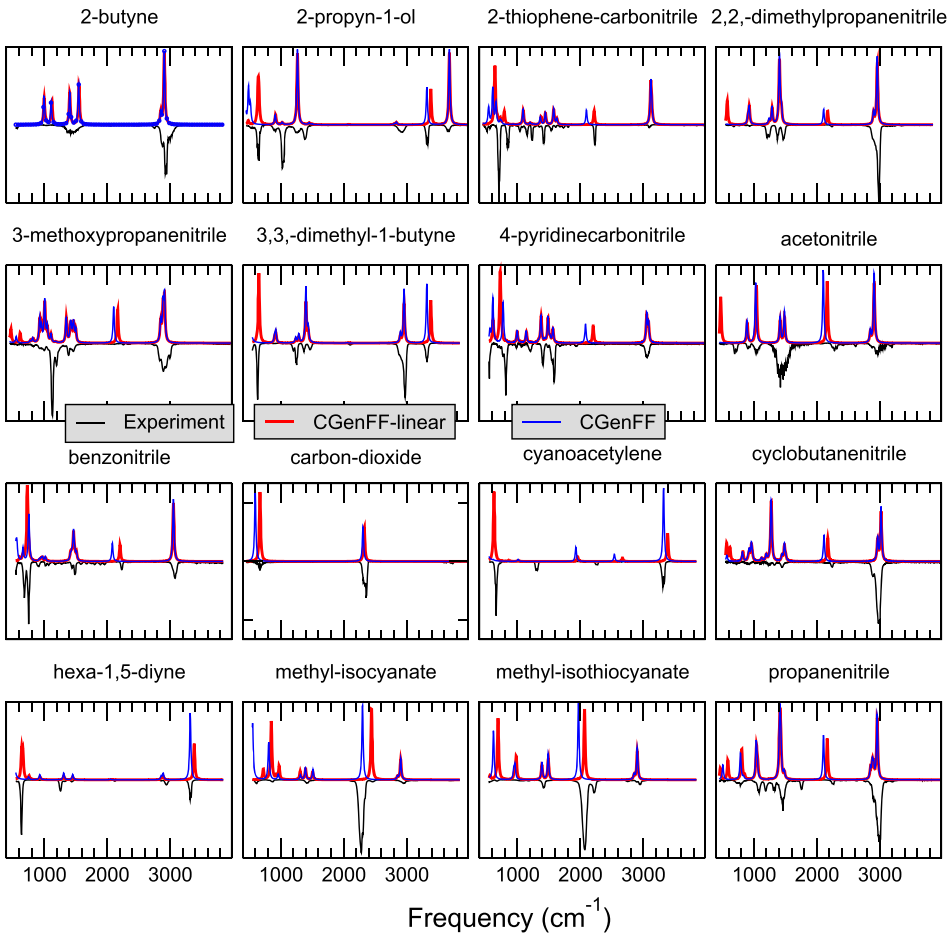

FIG. 2. Infrared spectra for all compounds computed according to the procedure described by Henschel *et al.*[18] Intensities of the experimental spectra are depicted as negative.

TABLE III. Standard entropy S^0 and heat capacity at constant volume C_V (J/mol K) for the 16 compounds in this study. For reference, the results from quantum-chemical calculations at the G4 level of theory are included.[16,17]

	Expt.	G4	Linear	Traditional	Expt.	G4	Linear	Traditional
Compound	S^0 (J/mol K)				C_V (J/mol K)			
2-butyne	283.2[40]	304.0	355.8	345.4	69.5[16]	73.0	72.0	74.2
2-propyn-1-ol	293.3[40]	286.6	289.3	297.0	64.5[16]	66.3	67.6	72.4
2-thiophene-carbonitrile		323.6	321.2	324.2		87.7	85.2	88.5
2,2-dimethylpropanenitrile	331.2[40]	339.4	337.8	341.9	116.2[16]	110.4	111.1	113.5
3-methoxypropanenitrile	364.4[40]	343.7	341.8	346.0	98.7[16]	95.7	98.0	100.4
3,3-dimethyl-1-butyne	335.7[40]	343.7	346.2	353.9	115.2[16]	119.2	121.3	126.1
4-pyridinecarbonitrile		327.0	329.5	332.8		92.7	97.4	100.7
Acetonitrile	242.6[40]	242.1	240.5	244.9	43.9[16]	43.0	42.0	44.7
Benzonitrile	321.5[40]	322.6	320.4	323.6	100.7[16]	97.0	95.6	98.9
Carbon dioxide	213.7[41]	207.7	213.7	214.9	28.9[16]	28.4	28.7	30.4
Cyanoacetylene		248.4	244.7	254.9	56.3[16]	54.1	49.4	57.6
Cyclobutanenitrile		315.4	308.3	312.8		85.4	83.6	86.2
Hexa-1,5-diyne		335.9	334.8	350.9		101.3	101.4	110.9
Methyl-isocyanate	195.5[41]	293.2	288.2	290.9	44.8[16]	54.8	54.7	58.4
Methyl-isothiocyanate		313.3	300.3	303.7		60.1	59.5	63.1
Propanenitrile	285.4[40]	284.4	281.1	285.4	65.5[16]	62.7	61.5	63.9

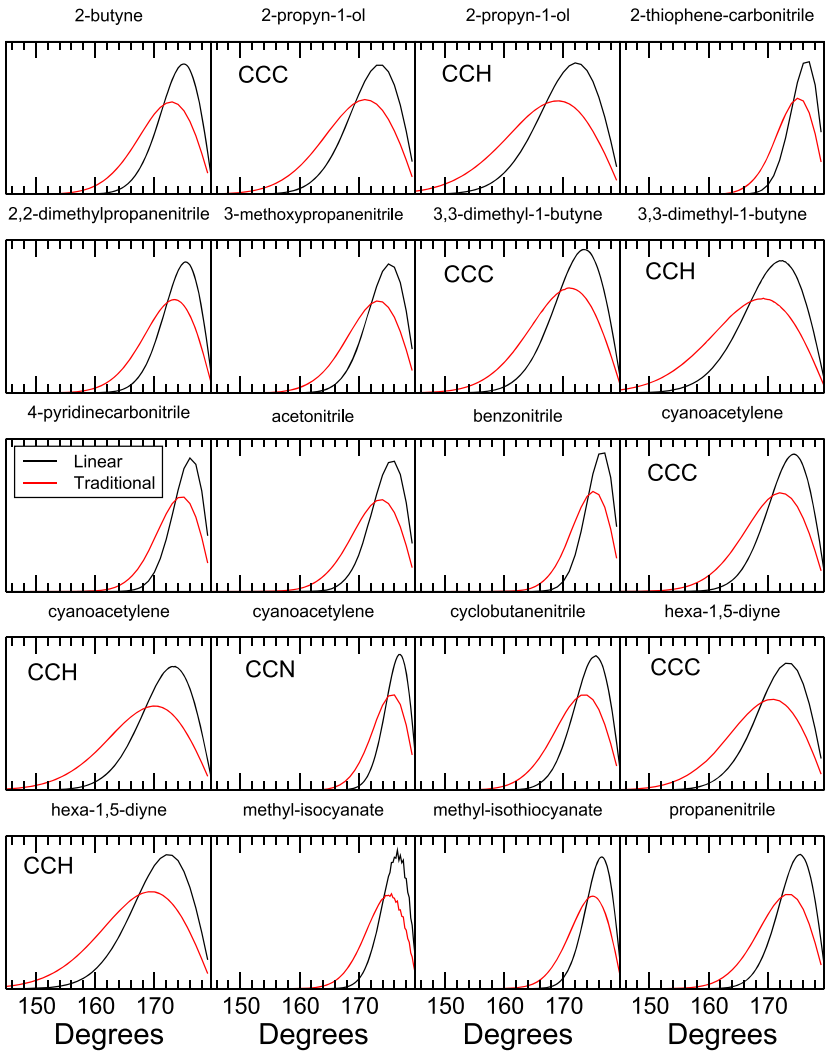

FIG. 3. Angle distribution functions for all linear groups in all compounds, averaged over the last 10 ns of a 20 ns simulation.

approaches are small, but it seems that there is a small increase in the density when using the linear angle potential. The enthalpy of vaporization for the 15 compounds is listed in Table S3. The difference between the potential models is small in all cases. Although the focus in this paper is on the development of a new potential rather than validation of a force field, it is worth noting that the liquid density and the enthalpy of vaporization are close to the experimental values in most cases.

D. Liquid carbon dioxide

Simulations of liquid carbon dioxide were performed at three different pressures, 50 bars, 100 bars, and 200 bars, and at two temperatures, 225 K and 250 K, covering a significant part of the liquid phase diagram. Figure 4 summarizes the properties of the model. We found that simulations with a Lennard-Jones cutoff of 1.1 nm plus analytical corrections (see Sec. III) were unstable, fluctuating between very high and low density. This is a well-known feature of the Parrinello–Rahman pressure coupling method[42] that signifies problems with the physical model. When using the Lennard-Jones PME (LJ-PME) method[30] that was implemented in GROMACS recently,[32] the simulations were stable and converged to the properties in Fig. 4. In order to investigate this further, we performed additional long MD simulations using cutoffs of 1.4 nm, respectively, 1.7 nm plus analytical corrections. Table S1 lists the density, potential energy, and diffusion constants D of the CO_2. In all cases, the systems are stable and in the liquid state ($D > 0$). However, the density using a 1.4 nm cutoff is found to be 50 g/l–100 g/l higher, the potential energy lower, and diffusion retarded. Inspection of the C–C radial distribution function (RDF, Fig. S1) shows that the liquid is structured beyond the cutoff of 1.4 nm and even 1.7 nm. The differences between RDFs from simulations with a cutoff and with LJ-PME are large (Fig. S2), showing that the cutoff induces extra structure in the liquid.

It has previously been found that LJ-PME has a large influence on the behavior of systems with interfaces such as biological

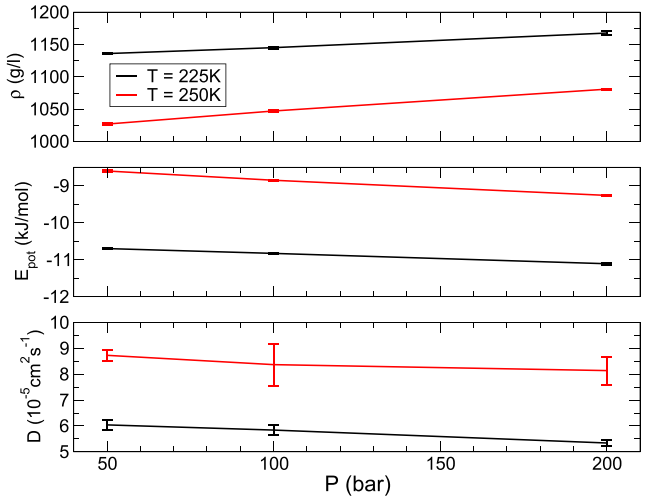

FIG. 4. Properties of liquid CO_2 using the linear potential and LJ-PME.

membranes[32] or liquid–vacuum interfaces.[10] Indeed, it is well established that electrostatics cutoffs can lead to ordering in liquids[43] and even spurious phase transitions (see van der Spoel and van Maaren[44] for an in-depth discussion). For pure homogeneous liquids, it was expected that the somewhat costly LJP-ME method would not be needed and that analytical corrections to energy and pressure[31] would be sufficiently accurate for faithful simulations. However, for the case of flexible carbon dioxide, we here report that due to significant ordering of the liquid phase at high pressure, even beyond the cutoff of even 1.4 nm (Fig. S1). Therefore, LJ-PME is a more rigorous option to describe liquid carbon dioxide as well. It is questionable whether simulation without LJ-PME models molecular energetics sufficiently accurately in general. Earlier simulations of liquid carbon dioxide used rigid models,[45–49] which may influence phase behavior. A fully flexible model was presented as well,[50] but this was only used in constant volume simulations. A very recent flexible model[51] for CO_2 was developed with much higher charges than what is used here and in most other published models, reducing the relative importance of the Van der Waals interactions. Interestingly, in Ref. 51, the cutoff used was 2.3 nm.

Liquid density for carbon dioxide as a function of temperature and pressure is given in Table IV. There seems to be some discrepancy between the NIST WebBook[52] and a relatively recent measurement series[53] with our simulation results, independent of the model, closer to the latter.

Having done simulations as a function of pressure allows us to compute the isothermal compressibility κ_T according to

$$\kappa_T = -\frac{1}{V}\frac{\partial V}{\partial P} \tag{17}$$

and compare both models. κ_T and ΔH_{vap} for carbon dioxide are given in Table V computed by first extrapolating the potential energy *Epot* in the liquid simulations to the saturation vapor pressure P = 7.2 bars (225 K) and 17.5 bars (250 K), and then using

TABLE IV. Liquid density obtained for CO_2 for the modified CGenFF with the linear potential and for traditional CGenFF. Experimental data from Velasco *et al.*[53] at T = 253.15 K.

		Density (kg/m^3)			
T (K)	P (bars)	Linear	Traditional	Experiment	
225	50	1135.9(0.9)	1138.6(0.8)	1157.7[52]	
225	100	1145.1(2)	1150.1(0.7)	1168.6[52]	
225	200	1167.7(4)	1169.6(0.7)	1188.0[52]	
250	50	1026.9(3)	1031.3(1.1)	1058.9[52]	1044.83[53]
250	100	1047.1(1.1)	1052.8(1.0)	1076.4[52]	1063.82[53]
250	200	1080.9(0.9)	1081.5(0.9)	1105.5[52]	1094.47[53]

TABLE V. Isothermal compressibility κ_T (10^{-4}/bar) and enthalpy of vaporization ΔH_{vap} for CO_2 for the modified CGenFF with the linear potential and for traditional CGenFF. Experimental data from Velasco *et al.*[53] at T = 253.15 K.

	T (K)	Linear	Traditional	Experiment
κ_T	225	1.9(0.1)	2.0(0.2)	
κ_T	250	3.4(0.5)	2.9(0.2)	3.26[53]
ΔH_{vap}	225	16.2(0.1)	15.5(0.1)	
ΔH_{vap}	250	14.6(0.1)	13.9(0.1)	12.72[41]

$$\Delta H_{vap} = (Epot(g) + k_B T) - Epot(l), \tag{18}$$

where (g) and (l) denote the gas and liquid phases, respectively, and k_B is the gas constant. Saturation pressures were computed using the Antoine equation.[54] The simulated density as a function of pressure at T = 250 K, the κ_T, and the Δh_{vap} are all close to recently measured experimental data,[53] highlighting that the intermolecular force field from CGenFF[15,23,24] is reasonably accurate when used in conjunction with explicit long range Lennard-Jones interactions.[30,32]

V. CONCLUSION

In this work, we have introduced a new potential for bending of linear compounds and evaluated the gas- and liquid-phase properties of 16 compounds. A simple analytical equation allows us to convert traditional force fields for linear compounds to the equations introduced here on the fly when starting a simulation. The properties of the 16 compounds are very similar to those of the original force field, as expected. By tuning the force constants, we found that it was straightforward to reproduce the observed frequencies for carbon dioxide. To improve the intermolecular force field for carbon dioxide for use in, e.g., simulations of carbon sequestration[55] or a biological context,[56,57] additional work may be needed.

The major advantage of the new potential [Eq. (7)] is that angles are maintained slightly closer to 180° than the traditional potential. It is also slightly less computationally expensive than the traditional potential [Eq. (1)] or than implementations using virtual sites. Finally, it should be stressed that the new potential is a harmonic function of the atomic coordinates, rather than of the angle.

Replacing a 180° conventional angle potential [Eq. (1)] by a linear angle potential [Eq. (7)] may influence other vibrational frequencies in the molecule. This may therefore necessitate tuning of other force constants in order to reproduce experimental vibrational frequencies, as we have done here for the case of carbon dioxide where the introduction of an additional O–O harmonic coupling enabled us to reproduce all four frequencies quantitatively.

SUPPLEMENTARY MATERIAL

See the supplementary material for the effect of a Lennard-Jones cutoff on simulations of liquid carbon dioxide and the effect of pressure scaling algorithms on liquid density for other compounds. Furthermore, there are tables of the average density of liquids, the enthalpy of vaporization, and the average angle of linear moieties using traditional and linear angle potentials. Finally, the results from free energy perturbation calculations are given.

ACKNOWLEDGMENTS

The Swedish Research Council is acknowledged for a grant of computer time (Grant No. SNIC2018-2-42). Funding from eSSENCE—The e-Science Collaboration (Uppsala-Lund-Umeå, Sweden) is gratefully acknowledged.

DATA AVAILABILITY

The data that support the findings of this study are openly available from the GROMACS molecule & liquid database[9] at http://virtualchemistry.org.

REFERENCES

[1] J. Wang, W. Wang, P. A. Kollman, and D. A. Case, J. Mol. Graphics Mod. **25**, 247260 (2006).
[2] D. van der Spoel, E. Lindahl, B. Hess, G. Groenhof, A. E. Mark, and H. J. C. Berendsen, J. Comput. Chem. **26**, 1701 (2005).
[3] B. Hess, C. Kutzner, D. Van der Spoel, and E. Lindahl, J. Chem. Theory Comput. **4**, 435 (2008).
[4] D. van der Spoel and B. Hess, Wiley Interdiscip. Rev.: Comput. Mol. Sci. **1**, 710 (2011).
[5] S. Pronk, S. Páll, R. Schulz, P. Larsson, P. Bjelkmar, R. Apostolov, M. R. Shirts, J. C. Smith, P. M. Kasson, D. van der Spoel, B. Hess, and E. Lindahl, Bioinformatics **29**, 845 (2013).
[6] K. A. Feenstra, B. Hess, and H. J. C. Berendsen, J. Comput. Chem. **20**, 786 (1999).
[7] D. van der Spoel, M. M. Ghahremanpour, and J. A. Lemkul, J. Phys. Chem. A **122**, 8982 (2018).
[8] C. Caleman, P. J. van Maaren, M. Hong, J. S. Hub, L. T. Costa, and D. van der Spoel, J. Chem. Theory Comput. **8**, 61 (2012).
[9] D. van der Spoel, P. J. van Maaren, and C. Caleman, Bioinformatics **28**, 752 (2012).
[10] N. M. Fischer, P. J. van Maaren, J. C. Ditz, A. Yildirim, and D. van der Spoel, J. Chem. Theory Comput. **11**, 2938 (2015).
[11] J. Zhang, B. Tuguldur, and D. van der Spoel, J. Chem. Inf. Model. **55**, 1192 (2015).
[12] J. Zhang, B. Tuguldur, and D. van der Spoel, J. Chem. Inf. Model. **56**, 819 (2016).
[13] J. Wang, R. M. Wolf, J. W. Caldwell, P. A. Kollman, and D. A. Case, J. Comput. Chem. **25**, 1157 (2004).
[14] W. L. Jorgensen and J. Tirado-Rives, Proc. Natl. Acad. Sci. U. S. A. **102**, 6665 (2005).
[15] K. Vanommeslaeghe, E. Hatcher, C. Acharya, S. Kundu, S. Zhong, J. Shim, E. Darian, O. Guvench, P. Lopes, I. Vorobyov, and A. D. Mackerell, Jr., J. Comput. Chem. **31**, 671 (2010).
[16] M. M. Ghahremanpour, P. J. van Maaren, J. C. Ditz, R. Lindh, and D. van der Spoel, J. Chem. Phys. **145**, 114305 (2016).
[17] M. M. Ghahremanpour, P. J. van Maaren, and D. van der Spoel, Sci. Data **5**, 180062 (2018).
[18] H. Henschel, A. T. Andersson, W. Jespers, M. Mehdi Ghahremanpour, and D. van der Spoel, J. Chem. Theory Comput. **16**, 3307 (2020).
[19] H. Henschel and D. van der Spoel, J. Phys. Chem. Lett. **11**, 5471 (2020).
[20] P. M. Chu, F. R. Guenther, G. C. Rhoderick, and W. J. Lafferty, J. Res. Natl. Inst. Stand. Technol. **104**, 59 (1999).
[21] S.-N. Huang, T. A. Pascal, W. A. Goddard III, P. K. Maiti, and S.-T. Lin, J. Chem. Theory Comput. **7**, 1893 (2011).
[22] P. J. Linstrom and W. G. Mallard, *NIST Chemistry WebBook: NIST Standard Reference Database Number 69* (NIST, 2011), http://webbook.nist.gov.
[23] K. Vanommeslaeghe and A. D. MacKerell, Jr., J. Chem. Inf. Model. **52**, 3144 (2012).
[24] K. Vanommeslaeghe, E. P. Raman, and A. D. MacKerell, Jr., J. Chem. Inf. Model. **52**, 3155 (2012).
[25] M. M. Ghahremanpour, P. J. van Maaren, and D. van der Spoel (2017). "Alexandria Library [Data set]," Zenodo. https://doi.org/10.5281/zenodo.1170597
[26] M. J. Frisch, G. W. Trucks, H. B. Schlegel, G. E. Scuseria, M. A. Robb, J. R. Cheeseman, G. Scalmani, V. Barone, G. A. Petersson, H. Nakatsuji, X. Li, M. Caricato, A. V. Marenich, J. Bloino, B. G. Janesko, R. Gomperts, B. Mennucci, H. P. Hratchian, J. V. Ortiz, A. F. Izmaylov, J. L. Sonnenberg, D. Williams-Young, F. Ding, F. Lipparini, F. Egidi, J. Goings, B. Peng, A. Petrone, T. Henderson, D. Ranasinghe, V. G. Zakrzewski, J. Gao, N. Rega, G. Zheng, W. Liang, M. Hada, M. Ehara, K. Toyota, R. Fukuda, J. Hasegawa, M. Ishida, T. Nakajima, Y. Honda, O. Kitao, H. Nakai, T. Vreven, K. Throssell, J. A. Montgomery, Jr., J. E. Peralta, F. Ogliaro, M. J. Bearpark, J. J. Heyd, E. N. Brothers, K. N. Kudin, V. N. Staroverov, T. A. Keith, R. Kobayashi, J. Normand, K. Raghavachari, A. P. Rendell, J. C. Burant, S. S. Iyengar, J. Tomasi, M. Cossi, J. M. Millam, M. Klene, C. Adamo, R. Cammi, J. W. Ochterski, R. L. Martin, K. Morokuma, O. Farkas, J. B. Foresman, and D. J. Fox, Gaussian 16 Revision A.03, Gaussian, Inc. Wallingford, CT, 2016.
[27] J. M. Martínez and L. Martínez, J. Comput. Chem. **24**, 819 (2003).
[28] L. Martínez, R. Andrade, E. G. Birgin, and J. M. Martínez, J. Comput. Chem. **30**, 2157 (2009).
[29] B. Hess, J. Chem. Theory Comput. **4**, 116 (2008).
[30] U. Essmann, L. Perera, M. L. Berkowitz, T. Darden, H. Lee, and L. G. Pedersen, J. Chem. Phys. **103**, 8577 (1995).
[31] M. P. Allen and D. J. Tildesley, *Computer Simulation of Liquids* (Oxford Science Publications, Oxford, 1987).
[32] C. L. Wennberg, T. Murtola, B. Hess, and E. Lindahl, J. Chem. Theory Comput. **9**, 3527 (2013).
[33] S. Nosé, Mol. Phys. **52**, 255 (1984).
[34] W. G. Hoover, Phys. Rev. A **31**, 1695 (1985).
[35] M. Parrinello and A. Rahman, J. Appl. Phys. **52**, 7182 (1981).
[36] H. J. C. Berendsen, J. P. M. Postma, W. F. van Gunsteren, A. DiNola, and J. R. Haak, J. Chem. Phys. **81**, 3684 (1984).
[37] G. Bussi, D. Donadio, and M. Parrinello, J. Chem. Phys. **126**, 014101 (2007).
[38] W. L. Jorgensen, J. Chandrasekhar, J. D. Madura, R. W. Impey, and M. L. Klein, J. Chem. Phys. **79**, 926 (1983).
[39] P. Dauber-Osguthorpe and A. T. Hagler, J. Comput.-Aided Mol. Des. **33**, 133 (2019).
[40] C. L. Yaws, *Yaws' Handbook of Thermodynamic Properties for Hydrocarbons and Chemicals* (Knovel, 2009), http://www.knovel.com.
[41] R. L. Rowley, W. V. Wilding, J. L. Oscarson, Y. Yang, and N. F. Giles, *Data Compilation of Pure Chemical Properties* (Design Institute for Physical Properties; American Institute for Chemical Engineering, New York, 2012).
[42] E. Lindahl, B. Hess, and D. Van Der Spoel, J. Mol. Model. **7**, 306 (2001).
[43] Y. Yonetani, Chem. Phys. Lett. **406**, 49 (2005).

[44]D. van der Spoel and P. J. van Maaren, J. Chem. Theory Comput. **2**, 1 (2006).
[45]J. G. Harris and K. H. Yung, J. Phys. Chem. **99**, 12021 (1995).
[46]S. Tsuzuki and K. Tanabe, Comput. Mater. Sci. **14**, 220 (1999).
[47]J. J. Potoff and J. I. Siepmann, AIChE J. **47**, 1676 (2001).
[48]Z. Zhang and Z. Duan, J. Chem. Phys. **122**, 214507 (2005).
[49]J. Neuefeind, H. E. Fischer, J. M. Simonson, A. Idrissi, A. Schöps, and V. Honkimäki, J. Chem. Phys. **130**, 174503 (2009).
[50]A. Zhu, X. Zhang, Q. Liu, and Q. Zhang, Chin. J. Chem. Eng. **17**, 268 (2009).
[51]R. Fuentes-Azcatl and H. Domínguez, J. Mol. Model **25**, 146 (2019).
[52]E. W. Lemmon, M. O. McLinden, and D. G. Friend, "Thermophysical properties of fluid systems," in *NIST Chemistry WebBook: NIST Standard Reference Database Number 69*, edited by P. Linstrom and W. Mallard (National Institute of Standards and Technology, Gaithersburg, MD, USA, 2020).
[53]I. Velasco, C. Rivas, J. F. Martínez-López, S. T. Blanco, S. Otín, and M. Artal, J. Phys. Chem. B **115**, 8216 (2011).
[54]C. L. Yaws, *Antoine Equation and Coefficients for Inorganic Compounds* (Knovel, 2015).
[55]T. C. Lourenço, M. F. C. Coelho, T. C. Ramalho, D. van der Spoel, and L. T. Costa, Environ. Sci. Technol. **47**, 7421 (2013).
[56]K. M. Merz, Jr., J. Am. Chem. Soc. **113**, 406 (1991).
[57]M. van Lun, J. S. Hub, D. van der Spoel, and I. Andersson, J. Am. Chem. Soc. **136**, 3165 (2014).